ELSEVIER

Journal of Photochemistry and Photobiology A: Chemistry 108 (1997) 273–282

Journal of PHOTOCHEMISTRY AND PHOTOBIOLOGY A:CHEMISTRY

# Phthalocyanines bound to insoluble polystyrene. Synthesis and properties as energy-transfer photosensitizers

José L. Bourdelande [a], Mostafa Karzazi [a], Lelia E. Dicelio [b], Marta I. Litter [c], Gerard Marqués Tura [a], Enrique San Román [b,*], Velia Vinent [b]

[a] *Departamento de Química, Unidad de Química Orgánica, Universidad Autónoma de Barcelona, Bellaterra, 08193 Barcelona, Spain*
[b] *INQUIMAE, Facultad de Ciencias Exactas, Universidad de Buenos Aires, Pabellón II, Ciudad Universitaria, 1428 Buenos Aires, Argentina*
[c] *Unidad de Actividad Química, Comisión Nacional de Energía Atómica, Av. del Libertador 8250, 1429 Buenos Aires, Argentina*

Received 9 April 1996; accepted 21 February 1997

**Abstract**

Metallotetracarboxyphthalocyanines (MTCPc, M = Cu, Al) were bound to the amino groups of Amberlite IRA-93 by amide bonding. The insoluble materials obtained were characterized by IR absorption, visible absorption and diffuse reflectance, and ICP atomic emission spectroscopy, and tested for energy transfer under irradiation in the phthalocyanine Q-band. Samples containing AlTCPc are strongly fluorescent both in the solid state and in DMF suspension. Fluorescence quantum yields decrease sharply in toluene suspension. In the solid state, fluorescence may be quantitatively quenched by energy-transfer to an adsorbed dye. Singlet molecular oxygen ($^1O_2$) quantum yields were obtained in suspension by monitoring the photooxidation of diphenylisobenzofuran. Values are drastically reduced in DMF suspension and even more in toluene suspension relative to homogeneous solution. This fact is attributed to dye aggregation (M = Cu) and excited-state self-quenching (M = Al). Results can be rationalized by assuming that MTCPc incorporation occurs mainly at the polymer surface and that dye-to-dye interaction in suspension depends strongly on the environment. © 1997 Elsevier Science S.A.

*Keywords:* Fluorescence; Insoluble polymers; Phthalocyanines; Singlet molecular oxygen

## 1. Introduction

Phthalocyanines (Pcs), very stable dyes with strong absorption coefficients in the visible region (Q-band around 700 nm), are used as catalysts in several technological processes [1], as sensitizers in photobiological applications such as photodynamic therapy and inactivation of microorganisms [2–7], and in solar energy conversion [8,9]. Their photophysical and photochemical properties and photoredox activity have been extensively studied (see Ref. [8] and references cited therein).

Dye photoactivity may be modified by linkage to polymers soluble in water or polar solvents. Dyes can also be joined to insoluble polymers, with the advantage of their easy recovery from the reaction medium for subsequent reuse [10]. In particular, solid matrices are of great interest due to their potential to replace solid or soluble photosensitizers in the oil industry, laser technology, cancer therapy, etc.

Several routes have been investigated for linking dyes to polymers. Merrifield developed the so-called solid-phase synthesis for joining simple molecules to polymers (see Refs. [11,12] and references cited therein). This technique was used by Leznoff and coworkers to synthesize unsymmetrical Pcs [13,14] and earlier by Shaap et al. to obtain insoluble photosensitizers [15]. Previous work by one of us involved photophysical and photochemical studies of chromophores such as benzophenone and $Ru(bpy)_3^{2+}$ anchored to polystyrene beads [16–22]. Rose Bengal, pyrrole compounds, porphyrins and Pcs have been also anchored to or included into polymers [15,23–40]. In some cases, the photochemical reactivity of these systems was compared with that of isolated dyes [24–26,29,33,38] and, in other cases, their efficiency as singlet molecular oxygen ($^1O_2$) sensitizers has been tested [35,36,38–40].

Pcs substituted by carboxyl groups may be conveniently attached to different kinds of polymer via ester or amide links. Previous spectroscopic and photochemical studies of metallic tetracarboxyphthalocyanines (MTCPcs), especially on $^1O_2$ generation and charge-transfer reactions, have been performed by some of us in homogeneous and microheterogeneous media and their photophysical properties were correlated with the degree of aggregation [41–45]; it was dem-

* Corresponding author. Tel.: +54 1 782 0468; fax: +54 1 782 0441.


*PII* S1010-6030(97)00096-8

onstrated that cofacial dimers and higher oligomers neither fluoresce nor show photochemical activity in energy-transfer reactions, probably due to enhanced internal conversion.

In this paper we present the synthesis of polymeric materials composed of tetracarboxyphthalocyanines (MTCPc, M = Cu, Al) attached to Amberlite IRA-93 (**A**) and test their ability as energy-transfer photosensitizers in *N,N*-dimethylformamide (DMF) and in toluene suspension.

## 2. Experimental details

### 2.1. Chemicals

The polymeric support used was Amberlite IRA-93 (**A**, Fluka, see Fig. 1). This is a macroporous copolymer of styrene and *p*-aminostyrene cross-linked with DVB. To remove residual polymerization catalysts and other impurities commercial samples were purified by washing with dioxane, dioxane–0.1 N NaOH, dioxane–water, dioxane, dioxane–ethanol, dioxane–ethanol–ether, ethanol–ether and ether. Elemental analysis yielded 4.9 meq $NH_2$ $g^{-1}$ (58.3% functionalized phenyl groups).

MTCPcs (M = Cu, Al) were synthesized and purified as previously described, and characterized as the copper(II)-tetracarboxyphthalocyanine [42] and the hydroxyaluminumtricarboxymonoamidephthalocyanine [43]. 3,3′ − diethylthiatricarbocyanine iodide (DTTCI) and all other chemicals were commercial quality grade, and used without further purification. Solvents were spectrophotometric grade or carefully distilled and purified according to common techniques.

### 2.2. Analysis

Samples were characterized by elemental analysis and infrared, atomic, visible absorption and fluorescence spectroscopy. IR spectra, as KBr pellets, were taken on a Nicolet 5ZDX or on a Nicolet 510 P FTIR spectrophotometer. Inductively coupled plasma atomic-emission spectrometry (ICP-AES) was performed using an ICPAES Minitorch, ARL, model 3410. Visible spectra of suspended samples were recorded on a Shimadzu 160-A or on a Hewlett–Packard 8452A diode-array spectrophotometer. Diffuse-reflectance spectra of solid samples were obtained on a Shimadzu 210-A spectrophotometer equipped with an integrating sphere.

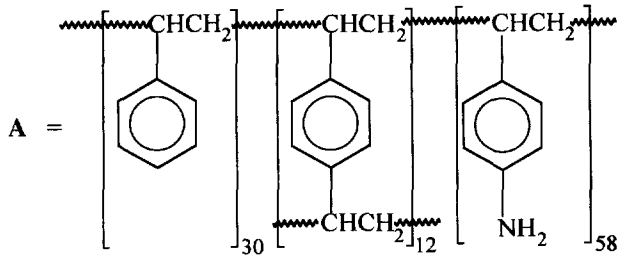


Fig. 1. The structure of Amberlite IRA-93.

Fluorescence spectra of suspended and solid-state samples were obtained on a Perkin–Elmer LS5 spectrofluorimeter.

### 2.3. Covalent linkage of CuTCPc and AlTCPc to Amberlite IRA-93: A–CuTCPc, Sample 1 and A–AlTCPc, Samples 2, 3, 4, and 5

The synthesis of Sample **1** is described. To 25.4 mg (0.034 mmol) CuTCPc in 35 mL anhydrous DMF, 76.7 mg polymer **A** ($M_0$: 118; 0.38 meq $NH_2$ groups), previously ground in an agate mortar, and 30.8 mg (0.15 mmol) dicyclohexylcarbodiimide (DCC) were added. The mixture was stirred at 120 °C for 96 h. After filtration, the powder was washed with the following series of solvents: DMF until colorless filtrate, DMF–dioxane, $CH_2Cl_2$, dioxane, dioxane–acetone, dioxane–acetone–ether, acetone–ether and ether. The dark blue polymer **1** was obtained.

Samples **2**–**5**, were similarly synthesized. Sample **2**: 16.5 mg AlTCPc (0.020 mmol), 51.2 mg **A** ($M_0$: 118; 0.25 meq $NH_2$ groups), 16.6 mg DCC, 12 mL DMF, 105 °C and 63 h (green powder). Sample **3**: 73.73 mg AlTCPc (0.101 mmol), 2.05 g **A** ($M_0$: 118; 10.13 meq $NH_2$ groups), 71 mg DCC, 205 mL DMF, 120 °C and 44 h (green powder). Sample **4**: 131 mg AlTCPc (0.178 mmol), 150 mg **A** ($M_0$: 118; 0.74 meq $NH_2$ groups), 78 mg DCC, 355 mL DMF, 120 °C and 62 h (green powder). Sample **5**: 40 mg AlTCPc (0.051 mmol), 524 mg **A** ($M_0$: 118; 2.59 meq $NH_2$ groups), 45 mg DCC, 120 mL DMF, 120 °C and 65 h (green powder).

IR analysis (KBr) of all samples yielded spectra similar to that shown in Fig. 2(a). Elemental analyses were not reproducible due to incomplete burning of the samples and are therefore not shown. The results of ICP-AES were: Sample **1**: Cu, 0.264% (0.042 meq Pc $g^{-1}$ polymer; 0.51% functionalized phenyl groups); Sample **2**: Al, 0.099% (0.037 meq Pc $g^{-1}$ polymer; 0.45% functionalized phenyl groups); Sample **3**: Al, 0.063% (0.023 meq Pc $g^{-1}$ polymer; 0.28% functionalized phenyl groups); Sample **4**: Al, 0.127% (0.047 meq Pc $g^{-1}$ polymer; 0.58% functionalized phenyl groups); Sample **5**: Al, 0.077% (0.029 meq Pc $g^{-1}$ polymer; 0.35% functionalized phenyl groups).

### 2.4. Preparation of suspensions and stability of samples

To obtain suspensions homogeneous in particle size, powders were ground in an agate mortar and passed through a 54-μm sieve. Coarser fractions were ground further, and the process repeated until the whole sample was ground to less than pore size. On suspension of freshly ground samples in DMF (a good solvent for MTCPcs) some Pc loss was evidenced after filtration by the detection of its characteristic absorption in the liquid phase. Ultrasonication and vigorous stirring also caused further damage. Small polymer fragments or eventually detached dye, together with very fine polymer particles, were removed by repeated washing with DMF until no absorption was detected in the liquid phase. Finally, samples were washed with water, ethanol and acetone, and dried

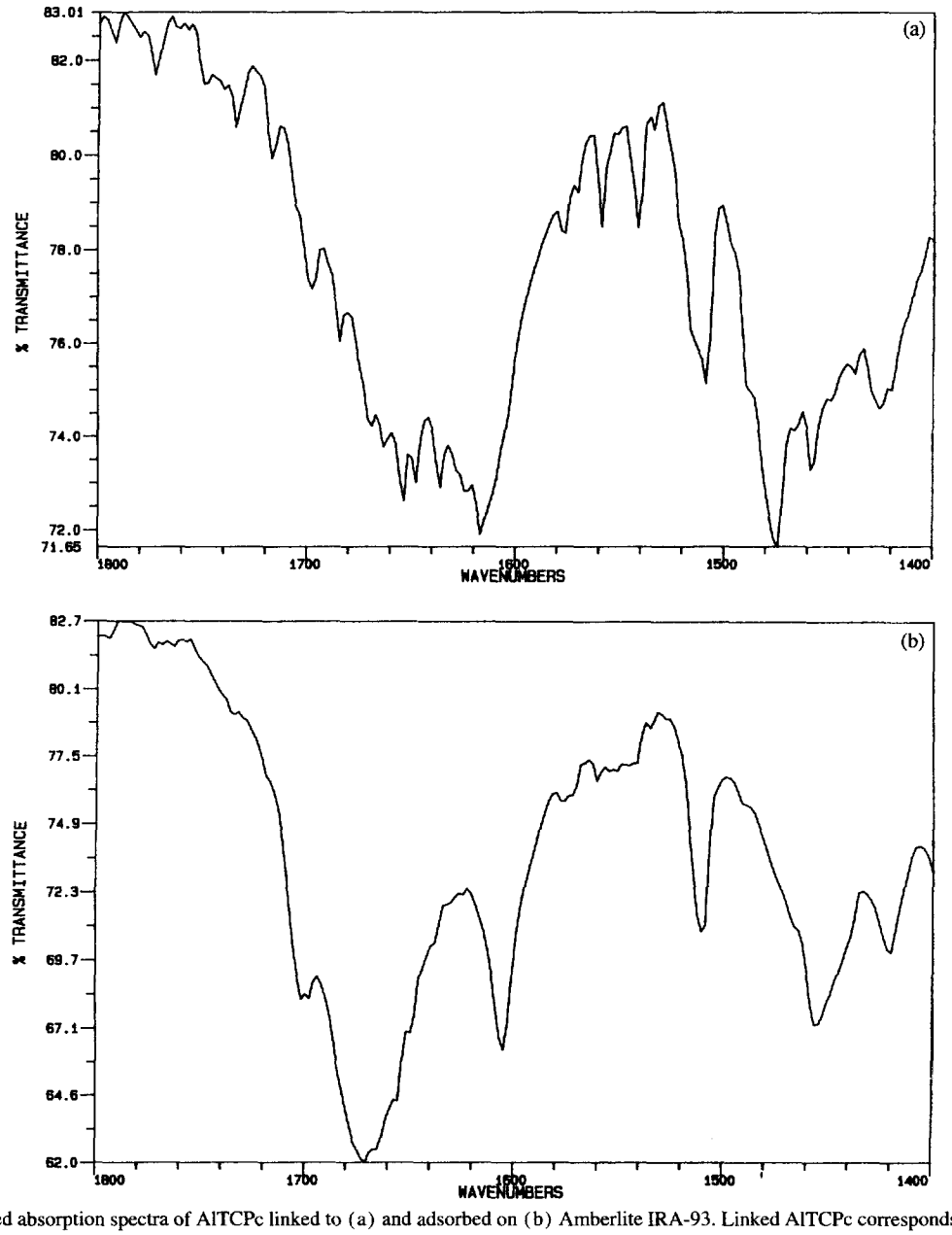


Fig. 2. Infrared absorption spectra of AlTCPc linked to (a) and adsorbed on (b) Amberlite IRA-93. Linked AlTCPc corresponds to Sample 3.

at 70 °C. Different solvents were tested to find the best medium to ensure a good wetting of the polymeric samples. DMF and toluene satisfied this condition, though moderate stirring was necessary to guarantee homogeneous dispersions.

After the foregoing treatment, polymers remained stable toward further washing with DMF, stirring, and irradiation with visible light. The obvious possibility that Pc was merely adsorbed on the polymer surface was discounted because weakly bound Pc should be easily removed with DMF. As it will be discussed later, experiments with adsorbed Pc as well as infrared spectroscopic evidence (Fig. 2) support this conclusion. On these grounds, ultrasonication and further grinding were avoided. Spectroscopic and irradiation measurements were carried out under stirring in DMF or toluene using freshly prepared suspensions, unless otherwise specified.

### 2.5. Spectroscopic measurements

Diffuse-reflectance spectra were recorded against MgO as neutral dispersant. Quantification of suspension extinction spectra required correction for background scattering. Efforts made to subtract scattering using a polymer suspension as the reference were not successful owing to baseline instability. Therefore, spectra were recorded against pure solvent and the scattering background was estimated by fitting the baseline to follow smoothly the zones where no dye absorption occurs. Previous stirring ensured proper suspension of samples.

Emission spectra of AlTCPc-containing polymer samples suspended in DMF were normally recorded after excitation at 620 nm. Absolute fluorescence quantum yields ($\phi_f$) were estimated relative to AlTCPc in solution in DMF. As this value was not known, it was calculated from that reported in dimethylsulfoxide (DMSO), $\phi_f = 0.42 \pm 0.02$ [43], taking into account the difference in the refractive index. The value obtained in DMF was 0.40. Absorbances of homogeneous solutions at the excitation wavelength were adjusted to the value of the suspensions corrected by scattering. $\phi_f$ was then calculated by integration of the emission spectra on a band 60 nm wide centered at the respective emission maximum. Within experimental error CuTCPc showed no fluorescence either in solution [43] or in polymeric samples.

Front-face fluorescence measurements were performed on solid polymeric samples immobilized on glass plates and luminescence quenching was studied in the solid state using adsorbed DTTCI as a quencher. For this purpose, 1.5–1.8 mg of polymer were homogeneously distributed on a 5 mm × 10 mm rectangle using double-sided sticky tape. Different amounts of DTTCI in 1:1 ethanol–acetone solution were then poured and solvent was allowed to evaporate. Final DTTCI masses were in the range $1 \times 10^{-10}$–$6 \times 10^{-8}$ mol. The excitation wavelength was 620 nm and fluorescence was detected between 650 and 800 nm using a cut-off filter (Schott RG645, thickness 3 mm). Blank tests were performed under different conditions. In particular, no fluorescence signals were detected on testing Amberlite without Pc in the presence of different amounts of DTTCI.

### 2.6. Singlet molecular oxygen photogeneration

Steady-state and time-resolved $^1O_2$ luminescence at 1.27 μm were measured on suspensions of polymeric samples in DMF and in toluene. In steady-state measurements, excitation at 670 nm was achieved by use of an Osram XBO, 450 W Xenon lamp and a monochromator (Sciencetech, 1200 lines $nm^{-1}$), following the luminescence signal by phase-sensitive detection with a lock-in EG & G PARC model 5105 amplifier. Pulsed-laser time-resolved experiments were performed using a Nd:YAG/dye laser combination Spectron Laser Systems model SL400, $\lambda_{exc} = 670$ nm, pulse width 8 ns. Maximum energies were 2.0 mJ $pulse^{-1}$. The unfocused beam was directed to a 10 mm × 10 mm fluorescence cuvette and emitted radiation was detected at right angles to the excitation beam. In both cases the detection system consisted of a 5-mm diameter germanium photodiode (Judson, J16-85P-R05M) fitted with a silicon filter and an interference filter at 1270 ± 10 nm (Silicon Filters and Spectrogon respectively). No $^1O_2$ luminescence was ever detected when dye-containing polymer samples were tested (in laser experiments the detection signal reached baseline level 2 μs after the excitation pulse). Previous experiments using a $N_2$ laser as excitation source ($\lambda_{exc} = 337.1$ nm, pulse width 8 ns) yielded similar results. Owing to the failure of luminescence experiments, chemical methods had to be used to detect and quantify $^1O_2$ photogeneration. Diphenylisobenzofuran (DPBF) was selected as chemical scavenger because it is soluble in DMF and in toluene. The decrease of its absorbance (corrected by polymer background scattering) was followed at 415 nm under steady-state polychromatic irradiation in the Pc Q-band (ca. 690 nm). Monochromatic irradiation was avoided because of low DPBF conversion rates, obscured by the scavenger thermal decomposition. The irradiation system was composed of a tungsten–halogen lamp (Phillips 24 V, 250 W) with a 665 nm cut-off filter (Schott RG665, thickness 3 mm) and a 100-mm path length water filter to avoid sample heating. The extinction of the polymer sample at the Q-band maximum was also followed to detect any dye detachment or bleaching. Pure solvent was used as a reference.

Typically, ca. 4 mg of Pc-containing polymer samples, weighed in a 10-mm path length absorption cell, were suspended in 3 mL DMF or toluene and solid DPBF was added to ensure 415 nm extinction values lower than 2.5 (the concentration of DPBF ranged from 70 to 100 μM). Final DPBF conversions were typically lower than 60% in DMF and much less in toluene, with photon fluxes between $1.2 \times 10^{-6}$ and $7.3 \times 10^{-6}$ M $s^{-1}$ $nm^{-1}$ (see Section 3, Results and Discussion) and reaction times of the order of 15–20 min. In most of the irradiation experiments, air-saturated suspensions were used. As in this case $[O_2] = 0.95 \times 10^{-3}$ M in DMF [46] and $1.73 \times 10^{-3}$ M in toluene [47], less than 11% of the initial amount of dissolved oxygen reacted with DPBF. In some experiments, oxygen or nitrogen was bubbled for several minutes before irradiation. Other experiments were performed with suspensions degassed at $10^{-5}$ torr after several freeze–pump–thaw cycles.

$\phi_\Delta$ values were obtained relative to AlTCPc in DMF. The reference value ($\phi_\Delta = 0.34$ for AlTCPc in DMF) was measured by standard procedures [43], using the 450-W Xenon lamp–monochromator combination as before at 680 ± 10 nm. The incident photon flux was $2.95 \times 10^{-5}$ M $s^{-1}$, calculated using a Gentec, Inc., Series PS-10 calibrated thermopile and a Keithley 193A digital multimeter.

Stability tests were performed to investigate any possible changes in the polymeric substrate as a result of irradiation (light or $^1O_2$ effects) or sample handling. For that purpose samples were irradiated for ca. 2 h in DMF under the same conditions as in the quantum-yield experiments, filtered, and tested for Pc absorption in the filtrate. The solid was washed with DMF, water, ethanol and acetone, dried, suspended, and irradiated again. In other experiments, DPBF was added initially to the suspensions, irradiation was performed for more than 2 h after $^1O_2$ photogeneration, DPBF (consumed after this time) was added again and its consumption rate was measured. Extinction spectra of previously irradiated samples were compared with those of freshly suspended polymers. No evidence of sample degradation was obtained and results of consecutive irradiation experiments on the same sample were fairly reproducible. No Pc was ever detected in the filtrates.

## 3. Results and discussion

### 3.1. Synthesis of polymer-bound phthalocyanines

CuTCPc and AlTCPc were attached to Amberlite joining the Pc-carboxyls to the polymer amino groups by amide links (see Scheme 1). IR spectra of polymer-bound Pcs were compared with those of samples prepared by adsorption of AlTCPc on Amberlite (see Fig. 2(a) and (b)). Free AlTCPc (not shown in the figure) shows an amide C=O band centered around 1660 $cm^{-1}$. This band, lying for adsorbed samples at nearly 1670 $cm^{-1}$, splits after attachment into two bands shifted to lower energies (approx. 1650 and 1620 $cm^{-1}$) and new bands attributable to a secondary amide appear at 1560 and 1540 $cm^{-1}$. These spectral changes demonstrate that dyes are effectively linked and not merely adsorbed or included into the polymer matrix.

The polymer samples obtained are summarized in Table 1 together with their spectral characterization. The degree of functionalization was calculated from the results of ICP-AES. It was always less than one Pc moiety per hundred monomer units, far less than the theoretically attainable functionality, though quite different starting amounts of Pc were used. Although a correlation does exist between starting amounts of Pc and final dye loadings (see Table 1, Samples **2–5**), it is evident that some kind of saturation effect does take place. Excessively long reaction periods at a high reaction temperature caused degradation and were therefore avoided.

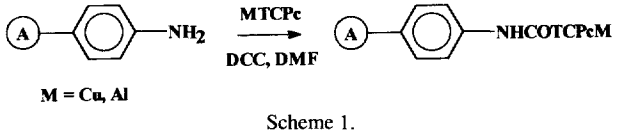


Scheme 1.

Low final degrees of functionalization can be understood assuming either that steric hindrance or multiple binding through different carboxyl groups of the same Pc restricts the entrance of the macrocycle into the polymeric matrix. Therefore, attachment should occur easily at the surface of the polymer beads and deeper penetration into the polymer network would be severely restricted. This restriction does not apply to linear polymers [26,29,31,38], for which larger loadings of Pcs and other macrocycles have been obtained. Previous work performed on benzoylated polystyrene beads and $Ru(bpy)_3^{2+}$ covalently bound to insoluble cross-linked polystyrene indicates that penetration of small dyes into the bulk polymer may occur, as evidenced by the differential photophysical behavior of dyes attached to the polymer surface and those included into the bulk polymer [16–22]. Interestingly, porphyrins seem to penetrate easily into the last polymer [34–36].

### 3.2. Visible spectra

In DMF solution AlTCPc shows a large peak at 684 nm ($Q_{0-0}$ band) with a shoulder at 650 nm ($Q_{0-1}$) and a smaller peak at 617 nm ($Q_{0-2}$). Spectra do not depend on concentration in the range $10^{-7}$–$10^{-4}$ M, indicating that dyes are in their monomeric form. Aggregation is promoted in aqueous alkaline solution, as demonstrated by the presence of a broad band reaching its maximum at approximately 640 nm with a height similar to the peak at the longer wavelength (ca. 690 nm) [41]. In contrast, the spectrum of CuTCPc in DMF depends strongly on concentration. At $5 \times 10^{-7}$ M, the monomeric form shows a large peak at 680 nm and a smaller one at 611 nm, whereas in more concentrated solutions a structureless band appears at 610–640 nm, which evolves at $3 \times 10^{-4}$ M into a broad band at approximately 630 nm of

Table 1
Composition of the Pc-bound polystyrenes and suspension absorption and diffuse reflectance spectra

| Sample | Type | $\%Pc_0^a$ | $\%Pc_f^b$ | mmol $g^{-1c}$ | $\lambda_{max}$ (nm) (relative intensities) | | |
|---|---|---|---|---|---|---|---|
| – | CuTCPc[d] | – | – | – | 611 (0.26) | – | 680 (1) |
| – | CuTCPc[e] | – | – | – | 630 (0.73) | – | 680 (1) |
| **1**[f] | A–Cu | 5.23 | 0.51 | 0.042 | 629 (1) | – | 690 (1) |
| – | AlTCPc | – | – | – | 617 (0.2) | 650 (shoulder) | 684 (1) |
| **2**[f] | A–Al | 4.65 | 0.45 | 0.037 | 620 (0.34) | 654 (0.7) | 691 (1) |
| **3**[f] | A–Al | 0.54 | 0.28 | 0.023 | 625 (0.17) | 652 (0.57) | 688 (1) |
| **3**[g] | A–Al | 0.54 | 0.28 | 0.023 | 625 (0.58) | 655 (0.74) | 690 (1) |
| **3**[h] | A–Al | 0.54 | 0.28 | 0.023 | 624 (0.4) | 654 (0.78) | 694 (1) |
| **4**[f] | A–Al | 13.10 | 0.58 | 0.047 | 620 (0.15) | 655 (0.55) | 698 (1) |
| **5**[f] | A–Al | 1.15 | 0.35 | 0.029 | 620 (0.18) | 656 (0.47) | 685 (1) |
| **5**[g] | A–Al | 1.15 | 0.35 | 0.029 | 625 (0.65) | 655 (0.81) | 690 (1) |

[a]Theoretically attainable functionality, calculated from the starting amount of Pc used as the percentage of total phenyl groups contained in the polymer.
[b]Final functionality as the percentage of total phenyl groups.
[c]Final incorporation (mmol Pc $g^{-1}$ polymer).
[d]$5 \times 10^{-7}$ M in DMSO.
[e]$3 \times 10^{-4}$ M in DMSO.
[f]DMF suspension.
[g]Diffuse reflectance.
[h]Toluene suspension.

similar height as the long-wavelength band [41]. The differences observed for the two compounds reflect the fact that CuTCPc is planar and not greatly influenced by solvent coordination, whereas AlTCPc has a bent structure and a hydroxyl group strongly bound to the metal. Therefore, aggregation is possible in CuTCPc by cofacial interaction of Pc moieties, but it is hindered in AlTCPc.

Observed extinction and diffuse reflectance spectra of polymer samples show features similar to those of the parent dyes, though complicated by background scattering and interaction with the matrix. Band broadening and slight changes in the position of the absorption maxima can be attributed to hydrogen bonding or to microenvironment fluctuations [26,29–31,34,38,40]. In contrast, aggregation effects, arising from a high local concentration of bound chromophores, are expected to be a source of profound spectral changes, as in homogeneous solution. Data for DMF suspension extinction and diffuse reflectance absorption spectra are shown in Table 1 together with the absorption maxima and relative absorbances for non-bound Pcs. As was expected, due to the cofacial interaction of Pc moieties already mentioned and to a high local concentration, **A**–CuTCPc (Sample **1**) shows a high extent of aggregation and, accordingly, it should be less efficient for $^1O_2$ photogeneration [42].

AlTCPc-containing polymers show quite different behavior. Though enhancement of absorption at lower wavelengths (620 nm) and appearance of a new band at 650 nm are observed in DMF and in toluene suspension, no spectral shifts are found relative to the homogeneous system (cf. AlTCPc and Samples **2**–**5** in Table 1). Therefore, spectral changes can be attributed to interactions between the dye and the polymeric support rather than to interactions among dye moieties.

### 3.3. Fluorescence spectra

**A**–Al samples fluoresce strongly in DMF with an emission maximum at 700 nm, which is very close to the value found for AlTCPc (698 nm) in the same solvent. The excitation spectra of polymeric samples resemble the absorption spectra of AlTCPc in DMF [43]. $\phi_f$ values are shown in Table 2. The fact that these values are of the same order as those found in homogeneous solution supports the conclusion that the extent of aggregation is not high in DMF. Toluene suspensions (**3**[d], Table 2) show a smaller $\phi_f$ value but, according to the essentially similar spectrum found in this solvent, this effect cannot be attributed to dye aggregation. An explanation of this behavior may be found by assuming that dyes are in closer contact in the last solvent, leading to some contribution of singlet state self-quenching (SSQ). The main difference between toluene and DMF is with regard to their affinity with AlTCPc. As toluene is a poor solvent for this compound, solvatophobic forces must enhance dye-to-dye interactions. This suggests a certain flexibility of dye linkage.

Solid-phase fluorescence-quenching measurements using DTTCI, acting as an energy-transfer quencher, were performed to gain some knowledge on the distribution of dyes in the polymer matrix. In Fig. 3 absolute fluorescence intensity measured at 700 nm (excitation at 620 nm) of Sample **3** is given as a Stern–Volmer plot. Linear behavior is observed showing that a sole quenching mechanism is effective. The relative fluorescence spectra are independent of the quencher mass (Fig. 4), though DTTCI absorption depends strongly on wavelength. This indicates that internal filtering is not likely to occur. This demonstrates that trivial energy transfer quenching does not take place. Furthermore, when the mass of quencher is increased sufficiently almost total fluorescence quenching is observed. These results indicate either that attached dyes are located on the polymer surface or, at least, that they can be easily accessed by the quencher.

Table 2
Fluorescence quantum yields ($\lambda_{exc}=620$ nm), singlet molecular oxygen quantum yields, and singlet oxygen quenching to decay rate constant ratio of homogeneous solutions and polymer samples in DMF (unless otherwise indicated)

| Sample | %$Pc_f$ | $\phi_f$ | $\phi_\Delta$ | $10^{-4}k_r/k_d$ ($M^{-1}$) |
|---|---|---|---|---|
| CuTCPc[a] | – | $<10^{-3}$ | $0.18\pm0.01$ | – |
| **1** | 0.51 | $<10^{-3}$ | $<10^{-4}$ | – |
| AlTCPc | – | 0.40 | $0.34\pm0.02$ | $3.1\pm1$ |
| **2** | 0.45 | | $0.043\pm0.005$ | $6.0\pm2$ |
| **3** | 0.28 | 0.29 | $0.032\pm0.004$ | $6.0\pm3$ |
| **3**[b] | 0.28 | | $0.043\pm0.005$ | $4.0\pm2$ |
| **3**[c] | 0.28 | | $0.053\pm0.005$ | $5.5\pm2$ |
| **3**[d] | 0.28 | 0.11 | $0.0050\pm0.0005$[e] | – |
| **3**[cd] | 0.28 | | $0.012\pm0.002$[e] | – |
| **4** | 0.58 | 0.38 | $0.043\pm0.005$ | $3.4\pm2$ |
| **5** | 0.35 | 0.26 | $0.064\pm0.005$ | $3.3\pm2$ |

[a]In DMSO, value corresponding to monomeric dye [43].
[b]Reused sample.
[c]Oxygen bubbling before irradiation.
[d]In toluene.
[e]Zero-order kinetics.

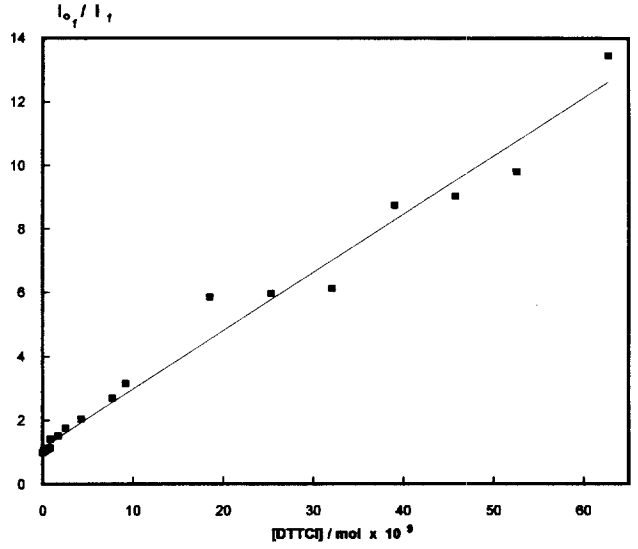


Fig. 3. Fluorescence intensity of polymer plates at 700 nm as a function of DTTCI mass; excitation at 620 nm.

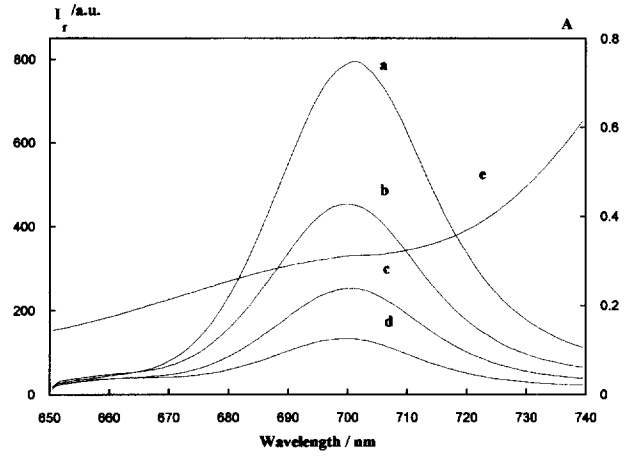


Fig. 4. Fluorescence spectra of polymer plates for different masses of DTTCI: 0 (a); $2.57\times10^{-9}$ (b); $9.19\times10^{-9}$ (c); and $32.1\times10^{-9}$ mol (d). Curve (e) represents the absorption spectrum of DTTCI $6.1\times10^{-6}$ M in ethanol.

### 3.4. Singlet molecular oxygen photogeneration

Detection of $^1O_2$ luminescence either by steady-state or time-resolved techniques failed, pointing to very low $\phi_\Delta$ values. Therefore, DPBF was used as $^1O_2$ monitor under steady-state irradiation. **A**–Al (Samples **2**–**5**) was effective in sensitizing DPBF consumption in the presence of molecular oxygen. No photochemical decomposition of DPBF was found using **A**–Cu (Sample **1**).

Assuming that DPBF is consumed exclusively by $^1O_2$, the following rate equation holds [41,42]:

$$-\frac{d[DPBF]}{dt}=-\frac{dA}{dt}\frac{1}{\epsilon_{DPBF}l}=I_a\phi_\Delta\frac{k_r[DPBF]}{k_r[DPBF]+k_d} \quad (1)$$

where $A$ is the absorbance of DPBF at 415 nm, $I_a$ is the total absorbed photon flux per unit volume and unit time, $\epsilon_{DPBF}$ is the molar absorption coefficient of DPBF in DMF or toluene at 415 nm ($2.2\times10^4$ $M^{-1}$ $cm^{-1}$ in both solvents, measured in this work), $l$ is the optical path length, $k_d$ is the $^1O_2$ decay rate constant and $k_r$ is the $^1O_2$ quenching rate constant by DPBF. Rearranging Eq. (1), it follows that:

$$-\left[\frac{dA}{dt}\right]^{-1}=\frac{1}{I_a\phi_\Delta\epsilon_{DPBF}l}+\frac{k_d}{k_rI_a\phi_\Delta}\frac{1}{A} \quad (2)$$

Plots of $(dA/dt)^{-1}$ versus $A^{-1}$ yield $I_a\phi_\Delta$ from the intercept and $k_r/k_d$ from the intercept-to-slope ratio. To calculate $I_a$, it must be taken into account that polychromatic irradiation ($\lambda\geq665$ nm) is used. Assuming that the incident photon flux per unit wavelength and unit volume, $I_0'=dI_0/d\lambda$, is a constant between the cut-off edge and 740 nm, where AlTCPc no longer absorbs, its value may be calculated from:

$$I_a=I_0'\int_{665\ nm}^{740\ nm}(1-10^{-A(\lambda)})d\lambda \quad (3)$$

where $A(\lambda)$ is the sample absorbance as a function of wavelength.

Used as an actinometer, AlTCPc was irradiated in homogeneous DMF solution containing DPBF under the same conditions as the polymeric samples. $I_a$ was calculated from the known value of $\phi_\Delta$ by use of Eq. (2) (see Section 2, Experimental details) and introduced in Eq. (3) to obtain $I_0'$. An advantage of this procedure is the similar spectral features of probe and actinometer. A similar approach was used to estimate $I_a$ for the polymeric samples once $I_0'$ was known. In this case the scattering background was deduced from the extinction spectra. Finally, $\phi_\Delta$ was calculated from the intercept in Eq. (2). According to the methodology just outlined, only light effectively absorbed by Pc is considered for the calculation of $\phi_\Delta$. Informed values, taken as a mean over several runs, are only approximate because the absorption spectrum of the dye in the polymeric sample is not the same as in homogeneous solution and, though light scattering is subtracted from the extinction spectra, true absorbances are difficult to evaluate in suspension. Results are however of comparative value.

The results obtained are summarized in Table 2 together with estimated errors arising essentially from dispersion of individual runs. Representative plots following Eq. (2) are given in Figs. 5 and 6. $\phi_\Delta$ values are much lower than in homogeneous solution [41,43] and, within the narrow range of concentrations involved, they do not correlate with the amount of incorporated Pc (cf. Samples **2**–**5**). These values are calculated at the actual oxygen pressure, corresponding either to air or oxygen saturation.

Copper samples do not yield $^1O_2$ within experimental error. This result is consistent with the spectral evidence already presented and suggests that formation of inactive aggregates inhibits energy-transfer to molecular oxygen, as previously found for dissolved CuTCPc [42].

$\phi_\Delta$ values obtained for aluminum samples are much lower than in homogeneous solution. Experiments carried out in toluene suspension show $\phi_\Delta$ values one order of magnitude lower than in DMF (cf. **3** and $\mathbf{3}^d$). Saturation with pure oxygen instead of air enhances $\phi_\Delta$ both in DMF and in toluene suspension to a certain extent (cf. **3** and $\mathbf{3}^d$ with $\mathbf{3}^c$ and $\mathbf{3}^{cd}$). Saturation with nitrogen has almost no effect on the photochemical DPBF consumption rate, but degassing of samples in a vacuum line inhibited this reaction quantitatively (results not shown). The last column in Table 2 gives the experimental $k_r/k_d$ ratios, as obtained from the intercept-to-slope ratio in Eq. (2). Within the large experimental error, these values do not differ appreciably from those observed in DMF solution. From the experiments carried out in toluene no information on $k_r/k_d$ is obtained, because zero-order kinetics are followed according to the long $^1O_2$ lifetime characteristic of this solvent.

As already discussed, aggregation does not seem to occur in aluminum samples and therefore it cannot be responsible for the lowering of $\phi_\Delta$. Excited-state self-quenching, already invoked to account for the lowering of fluorescence in toluene, provides an alternative explanation. Long-lived triplets are more sensitive to self-quenching than are singlet states,

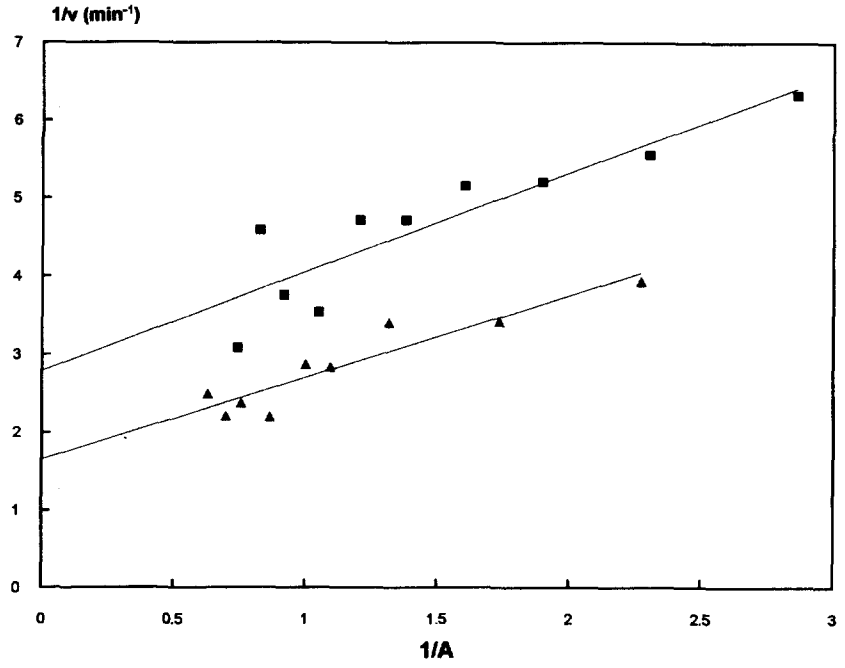


Fig. 5. Inverse DPBF decomposition rate versus inverse DPBF absorption. Sample **3** in DMF, mass = 3.8 mg, $[DPBF]_0 = 5.4 \times 10^{-5}$ M, photon flux = $6.96 \times 10^{-5}$ M min$^{-1}$ nm$^{-1}$, saturated with air (□) or oxygen (▽).

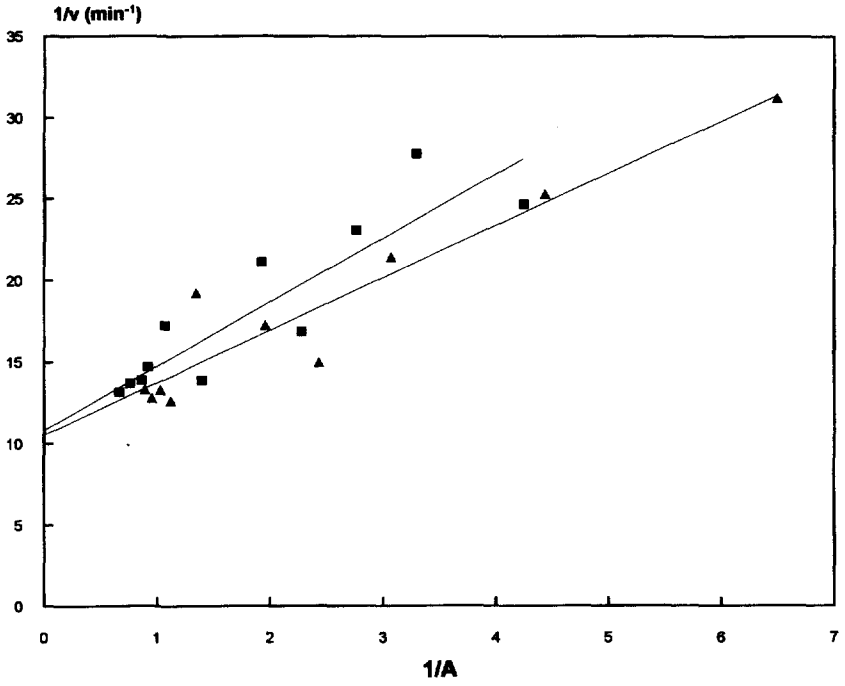


Fig. 6. Inverse DPBF decomposition rate versus inverse DPBF absorption. Sample **3** in DMF, mass = 4.2 mg, $[DPBF]_0 = 7.1 \times 10^{-5}$ M, photon flux = $4.04 \times 10^{-4}$ M min$^{-1}$ nm$^{-1}$, saturated with oxygen. Two tests under the same experimental conditions.

and this explains the overall lower $\phi_\Delta$ values [38,40]. In toluene, $\phi_\Delta$ decreases relatively to DMF as a result of both singlet- and triplet-self quenching (TSQ). The fact that toluene suspensions are far less efficient than DMF suspensions, despite higher oxygen solubility in the last solvent [46,47], can only be explained by assuming, as before, that toluene forces dye interaction, thus reducing $\phi_\Delta$ further. Diffusional constraints may be ruled out in view of the evidence obtained in solid-state fluorescence quenching experiments and the effect of oxygen pressure. Adsorbed DTTCI is able to quench every excited dye moiety when its surface concentration is increased sufficiently. In other words, as trivial energy-transfer is excluded, average distances between probe and quencher cannot exceed a few tens of nanometers. This means in turn, that either Pcs are at the polymer surface or DTTCI may diffuse freely into the bulk polymer. DPBF, being

smaller than DTTCI, would then be able to reach $^1O_2$ wherever it is formed. It is also hard to believe that molecular oxygen could be hindered from reaching the excited dyes. If this were the case, saturation with nitrogen or oxygen would have a pronounced effect on $\phi_\Delta$.

The results obtained point to the incorporation of Pc at or near the surface. Thus, the low degree of incorporation and its independence on the initial mass of dye, the results obtained from solid phase fluorescence, and the small effect of oxygen pressure are entirely consistent with this hypothesis. The homogeneity in the values of $k_r/k_d$ cannot either be considered as a thorough evidence that $^1O_2$ reacts with DPBF in the liquid phase rather than in the bulk polymer, but it does not contradict the assumption that only exposed areas of the polymer produce $^1O_2$ effectively. This fact also reinforces the hypothesis that this species is responsible for the oxidation of DPBF.

$\phi_\Delta$ values may be compared with those obtained by other authors. Schaap et al. obtained a value of 0.43 for Rose Bengal bound to an insoluble styrene–divinylbenzene copolymer (0.183 mmol dye $g^{-1}$ polymer), which should be compared with $\phi_\Delta = 0.76$ found for the same dye in methanol. Other sensitizers attached to the same polymer, namely fluorescein, chlorophyllin, and hematoporphyrin are nearly a factor of 10 less efficient [15]. The lowering of the ability of Rose Bengal to yield $^1O_2$ is far less important than in our case, though dye loadings are on the average six times larger than ours. The observed lowering could be attributed in principle to aggregation, self-quenching or diffusional constraints. Our results indicate that the low efficiency obtained for A–AlTCPc may be ascribed to a high surface concentration, which does not seem to occur in the case of Rose Bengal but may be important for the remaining dyes. Paczkowski and Neckers found in later work [40] that the efficiency of Rose Bengal attached to soluble poly(styrene–co–divinylbenzyl chloride) to sensitize singlet oxygen increases with the amount of attached dye, reaching a maximum at $\phi_\Delta \approx 0.4$, and decreases as the concentration of the dye further increases. The authors attribute the behavior found at low dye-loadings to the increase in solution viscosity with polymer mass and diffusion-controlled quenching of dye triplets by oxygen. Dye-to-dye interactions in the ground or excited states are invoked to explain the decrease observed at high dye loadings. Diffusion control is unlikely in our case, because dye moieties are available to oxygen at or near the surface of the polymer beads, where dye-to-dye interactions are very effective in reducing $\phi_\Delta$.

Ribó et al. [36] measured $\phi_\Delta$ for mesoporphyrin diesters bound to insoluble polystyrenes using bilirubin IX-$\alpha$ as $^1O_2$ quencher. Dye loadings were up to ten times higher than ours. They found that loadings larger than 0.05 mmol dye $g^{-1}$ polymer led to a dramatic reduction of $\phi_\Delta$, and they attributed this behavior to TSQ. Though no account is given of particle geometry, it is hard to believe that loadings as high as 0.3 mmol $g^{-1}$ may be accommodated at the polymer surface. Penetration of dyes into polymer beads was also suggested in the case of benzophenone attached to a polystyrene [20]. In this case, dye moieties are synthesized in situ by the Friedel–Crafts benzoylation of polystyrene and steric hindrance should be minimal. In our case, restricted diffusion of reactants during solid-state synthesis may be responsible for the preferential loading at the polymer surface.

## 4. Conclusions

Tetracarboxyphthalocyanines are attached preferentially at or near the surface of Amberlite IRA-93 leading to very high local concentrations of dye. Despite this, and because of their structural properties, aluminum phthalocyanines do not present evidence of dimerization, but self-quenching provides a rapid deactivation pathway for their triplet excited state. Singlet self-quenching may also arise when suspensions are prepared in poor phthalocyanine solvents. These materials seem to be not particularly suitable as photosensitizers for singlet molecular oxygen photogeneration, but may be active in driving energy or charge-transfer photoprocesses to adsorbed substrates.

## Acknowledgements

This work was financially supported by the Programa de Cooperación Científica con Iberoamérica (Ministerio de Educación y Ciencia de España y Agencia Española de Cooperación Internacional), the University of Buenos Aires, the Gesellshaft für Technische Zusammenarbeit, and the Volkswagen Foundation, Germany. We wish to thank Dr. Santiago Nonell (Instituto de Química de Sarriá, Barcelona, Spain) for his help on preliminary time-resolved singlet molecular oxygen luminescence experiments. ESR and MIL are members of the Consejo Nacional de Investigaciones Científicas y Técnicas (CONICET, Argentina).

## References

[1] F.H. Moser, A.L. Thomas, The Phthalocyanines, CRC Press Inc., Boca Raton, FL, 1983.
[2] J.D. Spikes, Photochem. Photobiol. 34 (1986) 691.
[3] I. Rosenthal, E. Ben-Hur, Phthalocyanines. Properties and Applications, VCH, NY, 1989, p. 393.
[4] J.R. Darwent, J. Mc Cubbin, G. Porter, J. Chem. Soc. Faraday Trans. 2: 78 (1982) 903.
[5] G. Jori, Photochem. Photobiol. 52 (1990) 439.
[6] G. Bertoloni, F. Rossi, G. Valduga, G. Jori, H. Ali, J. van Lier, Microbios 71 (1992) 33.
[7] G. Valduga, G. Bertoloni, E. Reddi, G. Jori, J. Photochem. Photobiol. B: Biol. 21 (1993) 81.
[8] J.R. Darwent, P. Douglas, A. Harriman, G. Porter, M.C. Richoux, Coord. Chem. Rev. 44 (1982) 83.
[9] S. Kimel, B.J. Tromberg, W.G. Roberts, M.W. Berns, Photochem. Photobiol. 50 (1989) 175.
[10] A.M. Braun, M.T. Maurette, E. Oliveros, Technologie Photochimique, Presses polytechniques romandes, Lausanne, 1986, p. 444.
[11] R.B. Merrifield, J. Am. Chem. Soc. 85 (1963) 2149.

[12] A. Akelah, A. Moet, Functionalized Polymers and their Applications, Chapman and Hall, London, 1990.
[13] C.C. Leznoff, T.W. Hall, Tetrahedron Lett. 23 (1982) 3023.
[14] T.W. Hall, S. Greenberg, C.R. Mc Arthur, B. Khouw, C.C. Leznoff, Nouv. J. Chim. 6 (1982) 653.
[15] A.P. Schaap, A.L. Thayer, E.C.Blossey, D.C. Neckers, J. Am. Chem. Soc. 97 (1975) 3741.
[16] J.L. Bourdelande, J. Font, F. Sánchez-Ferrando, Can. J. Chem. 61 (1983) 1007.
[17] F. Wilkinson, C.J. Willsher, J.L. Bourdelande, J. Font, J. Greuges, J. Photochem. 38 (1987) 381.
[18] J.L. Bourdelande, C. Campá, J. Camps, J. Font, P. De March, F. Wilkinson, C.J. Willsher, J. Photochem. Photobiol. A: Chem. 44 (1988) 51.
[19] J.L. Bourdelande, C. Campá, J. Font, P. De March, Eur. Polym. J. 25 (1989) 197.
[20] J.L. Bourdelande, J. Font, F. Wilkinson, C. Willsher, J. Photochem. Photobiol. A: Chem. 84 (1994) 279, and references cited therein.
[21] J.L Bordelande, J. Font, G. Marquès, D. Salvatierra, J. Photochem. Photobiol. A: Chem. 85 (1995) 143.
[22] J.L. Bourdelande, J. Font, in: J. Menon (Ed.), Trends Photochem. Photobiol., 3 (1994) 481.
[23] K. Hanabusa, X. Ye, T. Koyama, A. Kurose, H. Shirai, Makromol. Chem. 181 (1992) 575.
[24] H. Yamaguchi, R. Fujiwara, K. Kusuda, Makromol. Chem., Rapid Commun. 7 (1986) 225.
[25] H. Yamaguchi, R. Fujiwara, K. Kusuda, J. Macromol. Sci.-Chem. A24 (1987) 367.
[26] D. Wöhrle, G. Krawczyk, Makromol. Chem. 187 (1986) 2535.
[27] J. Gitzel, H. Ohno, E. Tsuchida, D. Wöhrle, Makromol. Chem., Rapid Commun. 7 (1986) 397.
[28] J. Gitzel, H. Ohno, E. Tsuchida, D. Wöhrle, Polymer 27 (1986) 1781.
[29] D. Wöhrle, J. Gitzel, G. Krawczyk, E. Tsuchida, H. Ohno, I. Okura, T. Nishizaka, J. Macromol. Sci.-Chem. A25 (1988) 1227.
[30] D. Wöhrle, G. Krawczyk, M. Paliuras, Makromol. Chem. 189 (1988) 1001.
[31] D. Wöhrle, T. Buck, G. Schneider, G. Schulz-Ekloff, H. Fischer, J. Inorg. Organomet. Polym. 1 (1991) 115.
[32] E. Giralt, J.M. Ribó, F.R. Trull, Tetrahedron Lett. 25 (1984) 4145.
[33] P. Castán, E. Giralt, J.C. Pérez, J.M. Ribó, N. Siscart, F.R. Trull, Tetrahedron 43 (1987) 2593.
[34] P. Castán, J.M. Ribó, F.R. Trull, Reactive Polymers 9 (1988) 237.
[35] J.M. Ribó, M.L. Sesé, F.R. Trull, in: G. Moreno, R.H. Pottier, J.G. Truscott (eds.), Photosensitization: Molecular, Cellular and Medical Aspects, NATO ASI Series, Vol. H15, Springer, Berlin, 1988, p. 361.
[36] J.M. Ribó, M.L. Sesé, F.R. Trull, Reactive Polymers 10 (1989) 239.
[37] Y.L. Zub, T.N. Yakubovich, A.B. Petcheny, K.A. Kolesnikova, Catal. Today 13 (1992) 691.
[38] J.D. Spikes, N.L. Krinick, J. Kopecek, J. Photochem. Photobiol. A: Chem. 70 (1993) 163.
[39] S. Nonell, M.L. Sesé, D.O. Mártire, S.E. Braslavsky, F.R. Trull, Photochem. Photobiol. 53 (1991) 185.
[40] J. Paczkowski, D.C. Neckers, Macromolecules 18 (1985) 1245.
[41] M.G. Lagorio, Ph.D. Thesis, University of Buenos Aires, 1991.
[42] M.G. Lagorio, L.E. Dicelio, E. San Román, S.E. Braslavsky, J. Photochem. Photobiol. B: Biol. 3 (1989) 615.
[43] M.G. Lagorio, L.E. Dicelio, E. San Román, J. Photochem. Photobiol. A: Chem. 72 (1993) 153.
[44] M.E. Daraio, P.F. Aramendía, E.A. San Román, S.E. Braslavsky, Photochem. Photobiol. 54 (1991) 367.
[45] R.M. Negri, A. Zalts, E.A. San Román, P.F. Aramendía, S.E. Braslavsky, Photochem. Photobiol. 53 (1991) 317.
[46] Du Pont de Nemours, Chem. Eng. News 33 (1955) 2366.
[47] IUPAC Solubility Data Series, R. Battino (Ed.) Vol. 5, Oxygen and Ozone, IUPAC, 1981.